ACS OMEGA

http://pubs.acs.org/journal/acsodf

Article

Two-Stage Supramolecular Self-Assembly-Directed Collagen-Peptide-Decorated Liposomal Complexes of Curcumin Microspheres with Enhanced Solubility and Bioavailability

Maria Jose Louis, Abhilash Balakrishnan, Ashil Joseph, Prasanth Shanmughan, Balu Maliakel, and Krishnakumar Illathu Madhavamenon*

Cite This: *ACS Omega* 2023, 8, 26243−26252

Read Online

ACCESS | Metrics & More | Article Recommendations | Supporting Information

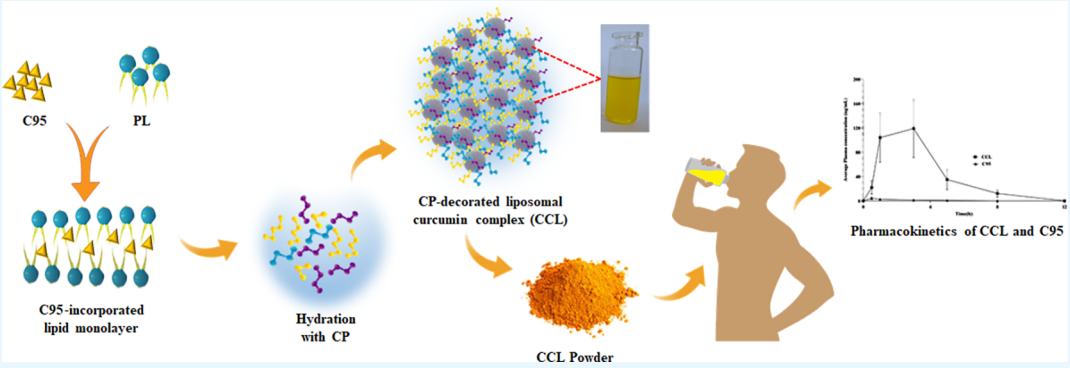

ABSTRACT: Green formulations of phytonutrients with enhanced solubility and bioavailability are of great significance in nutrition therapy. In the present contribution, we hypothesized that the collagen peptides could be a safe, natural, food-grade, and cost-effective functional agent for the surface decoration and stabilization of liposomes in powder form and hence a "green" solution for the oral delivery of phytonutrients. The present study reports a two-stage supramolecular self-assembly-directed process for the preparation of collagen peptide-decorated liposomal complexes of curcumin (CCL) [10% (w/w)] as microspheres (125 ± 25 μm) with improved solubility (1.46×10^5-fold) and sustained-release properties under gastrointestinal pH conditions. The molecular self-assembly of collagen peptides around the lipid bilayers and the various noncovalent interactions and conformational changes leading to the supramolecular assembly to act as a matrix for the encapsulation of lipid vesicles of curcumin were clear from the spectroscopic studies (UV−vis, fluorescence, FTIR, and circular dichroism). Further investigation of pharmacokinetics following a randomized double-blinded controlled trial on healthy volunteers (n = 15) demonstrated that the oral administration of 2.5 g of CCL sachet (250 mg of curcumin) enhanced the plasma concentration (C_{max}: 118 vs. 4.3 ng/mL), the elimination half-life (4.2 vs. 0.7 h), and bioavailability as per the area under the curve over 12 h [AUC_{0-12h} (CCL) = 506·8 vs. AUC_{0-12h} (C95) = 9.47 (53-fold)], when the plasma concentration of curcumin was estimated with triple quadruple tandem mass spectrometry (UPLC-ESI-MS/MS).

1. INTRODUCTION

Among the various drug delivery techniques, oral administration has been recognized as the most attractive route owing to the ease of administration, high adherence rate, sustained delivery, intensified immune response, long shelf-life, easy storage, and low cost of production.[1,2] However, oral delivery has been limited only to a few molecules since their physicochemical properties pose several hurdles with respect to insolubility, incompatibility, poor absorption, rapid biotransformation, rapid elimination (short systemic half-life), and hence low bioavailability and cellular uptake.[2,3] Several strategies have been reported to address the problems such as hydrophobicity, insolubility, crystallinity, and instability of low molecular weight bioactive molecules. However, formulations to minimize or prevent rapid intestinal/hepatic metabolism to allow the longer duration of existence of the bioactive forms of the active molecules in the systemic circulation at their therapeutically effective concentrations have yet to be identified.[2,4−6]

Liposomes are emerging as integral in nanomedicine, drug delivery, cosmetics, and food technology. The ability of

Received: April 13, 2023
Accepted: June 29, 2023
Published: July 11, 2023

amphiphilic lipids to self-assemble into a lipid bilayer-surrounded aqueous core to encapsulate both hydrophobic and hydrophilic molecules within their structures makes it attractive.[7] Liposomes improve the solubility and stability of encapsulated molecules with better bioavailability and cellular uptake including neurons.[8,9] However, oral delivery of liposomes has been shown to cause undesired payload seepage and degradation by the action of gastric acids, bile salts, and pancreatic lipases.[10] Liposomes also face the issues of their liquid state, especially the poor storage stability due to high free energy-directed aggregation and low drug loading capacity.[11] Among the various attempts to overcome the issues of liposomes, surface modification by synthetic polymers like polyethylene glycol and encapsulation in the hydrogel matrix have been shown to be promising.[12−14] In the present contribution, we hypothesized that the collagen peptides produced by the enzymatic hydrolysis of gelatin could be a natural, safe, food-grade, cost-effective, easily available, and functional agent for the surface decoration and stabilization of liposomes and hence would be a "green" solution to the limitations of liposomes. The study involved the development of a two-stage self-assembly process employing ethanol and water for the supramolecular rearrangement of collagen peptides, phospholipids (PL), and the bioactive molecules.

The process was illustrated using standard curcumin complex with >95% purity (C95) isolated from the rhizomes of turmeric (*Curcuma longa* L.) by solvent extraction. Curcumin, the yellow pigment in turmeric, has been identified as a potential antioxidant, anti-inflammatory, neuroprotective, and anti-proliferative phytonutrient with a pleiotropic mechanism of action to modulate multiple intracellular signaling pathways associated with cancer and neurodegenerative diseases.[15,16] However, it was found to exhibit limited clinical efficacy owing to its poor oral bioavailability contributed by its insolubility, hydrophobicity, in vivo instability, and extensive first-pass metabolism to inactive metabolites.[17] However, recent randomized controlled trials using enhanced bioavailable formulations have reported significant improvement in the anti-inflammatory efficacy of curcumin, especially toward joint pain, flexibility, and quality of life among osteoarthritic patients.[18] Collagen peptides on the other hand have shown to improve joint health (improve joint flexibility and reduce pain) due to its ability to enhance the synthesis of the extracellular matrix (ECM) and prevent the apoptosis of chondrocytes, in spite of its poor antioxidant and anti-inflammatory effects.[19] Therefore, we anticipated that the co-delivery of curcumin with collagen peptides in water-soluble and stable forms would improve the bioavailability and hence the clinical efficacy of collagen peptides, when delivered at their physiologically significant dosage.

Despite the chemical methods using synthetic emulsifiers and excipients, "green" approaches in addressing the poor bioavailability issues of phytonutrients are of great interest in nutritional therapy. The present contribution achieved supramolecular self-assembly of collagen peptides around the curcumin liposomes without using any synthetic excipients, and the subsequent—spray drying process generated a surface-decorated liposomal curcumin−collagen peptide complex (CCL) as sub-micronized particles with enhanced solubility, stability, and sustained release properties as characterized by various biophysical techniques. Plausible application of CCL as a functional food ingredient and dietary supplement was further evaluated by developing sachets and investigating the human pharmacokinetics following a randomized double-blinded protocol. Plasma curcumin concentrations at various post-administration time intervals were estimated by liquid chromatography−tandem mass spectrometry.

2. EXPERIMENTAL SECTION

2.1. Materials. Food-grade bovine collagen peptides (CPs) with an average molecular weight of 3000 Da were obtained from Nitta Gelatin India Limited, Cochin, India. Food-grade lecithin derived from sunflower seeds (PL) was obtained from Lipoid GmbH, Ludwigshafen, Germany. The natural curcuminoids complex with 95% purity [sum of curcumin, demethoxycurcumin (DMC), and bisdemethoxycurcumin (BDMC)] (C95) were extracted from turmeric rhizomes by extraction and crystallization with ethyl acetate and were obtained from Akay Natural Ingredients, Cochin, India.

2.2. Preparation of the CP−Curcumin Complex (CCL). About 11.2 g of curcumin was mixed with 4.6 g of medium chain triglyceride (MCT) oil and heated for 30 min to form a uniform mass. 11.2 g of lecithin was then dissolved in 50 mL of ethanol/water mixture and slowly added to curcumin mass with sonication, using a high-power ultrasound generator fitted with a sonotrode (1000 W), as pulses of 1−3 s (Hielscher Ultrasonics GmbH, Teltow, Germany). Ethanol was then evaporated under vacuum. About 73 g of CPs was separately dissolved in 400 mL of water, and the solution was slowly mixed with 275 mL of the curcumin−lecithin complex by high shear mixing. The solution was further homogenized at 600 bar pressure and dehydrated by spray drying (Labultima Process Technology Pvt. Ltd., Mumbai, India) to obtain CCL powder (yield: 93.6%; curcumin content: 10.2%).

Curcumin content was quantified by high-performance liquid chromatography (HPLC) (Nexera X2, LC-30AD), fitted with an SPD-M20A diode array detector (Shimadzu Analytical Private Limited, Kyoto, Japan), employing a reverse C18 column (250 × 4.6 mm, 5 μ), following a validated method (USP 35-NF 30, 2012, Page 1459). Analytical reference standards of curcumin (CAS# 458-37-7; purity ≥98%), DMC (CAS# 22608-11-3; purity ≥98%), and BDMC (CAS# 33171-05-0; purity ≥95%) were obtained from Sigma-Aldrich, Bangalore, India.

2.3. Characterization of CCL. Incorporation of curcumin into lipids and its further interaction with CPs were followed by solid-state Fourier-transformed infrared spectroscopy (FTIR), ultraviolet−visible (UV−vis) spectroscopy, and fluorescence spectroscopy. The conformational changes of CPs upon interaction with the curcumin−lipid complex were monitored by FTIR and circular dichroism (CD) spectroscopic studies. Powdered X-ray diffraction (PXRD) studies and differential scanning calorimetry (DSC) were employed to demonstrate the physical state and temperature stability of CCL. Scanning electron microscopy (SEM) provided information about the surface morphology and the encapsulation effect. The morphology of the particles in the solution was visualized under a transmission electron microscope (TEM), and particle size was measured by the dynamic light scattering (DLS) technique.

Solid-state FTIR spectra were recorded on a Thermo Nicolet iS50 spectrophotometer using potassium bromide pellets (Thermo Fisher Scientific, USA). Thirty-two scans per minute in the wavelength range 4000−400 cm^{-1} with a resolution of 4 cm^{-1} were taken for each sample. A thermogram was recorded using a differential scanning calorimeter (DSC) (Mettler-Toledo India Private Limited, Mumbai, India) by heating the

https://doi.org/10.1021/acsomega.3c02530
ACS Omega 2023, 8, 26243−26252

sample (3−5 mg) in the aluminum crimp pan at a rate of 10 °C/min from 30 to 300 °C under a nitrogen atmosphere. PXRD studies were performed on a Bruker D8 ADVANCE instrument: target Cu Kα 1.54 Å, filter Ni, voltage 40 kV, time constant 5 min/s, scanning rate 1°/min, and over a 2θ angle range of 10−90° (Bruker AXS GmbH, Karlsruhe, Germany). SEM analysis was done on SEM JEOL 6390 LA equipment (JEOL Limited, Tokyo, Japan). The particle size/zeta potential of CCL in solution was analyzed by a DLS equipment Horiba SZ-100 particle size analyzer (Horiba, Kyoto, Japan). The HR-TEM image of CCL was recorded on a JEOL JEM-2100 LaB6 HR-TEM (JEOL Co. Limited, Japan). CD data were collected in the wavelength range 190−300 nm using a CD spectropolarimeter and a quartz cuvette of 1 mm path length (JASCO 810, Tokyo, Japan). Electronic absorption spectra were recorded on a UV−vis spectrophotometer (UV-1900, Shimadzu, Tokyo, Japan) over the wavelength range of 200 to 500 nm at room temperature. The steady-state fluorescence spectra were recorded in a fluorescence spectrophotometer (Thermo Scientific, Varioskan LUX multimode microplate reader, Singapore).

2.4. Solubility and Encapsulation Efficiency. To measure the solubility, about 20 mg of curcumin (C95) or CCL was weighed into a 100 mL standard flask and made up with water (pH 7.4). The solution was sonicated in a bath sonicator for about 5 min to make sure the dissolution of the particles and centrifuged (3000 rpm for 5 min), and the supernatant was subjected to HPLC analysis to measure the dissolved curcumin content.[20]

In order to evaluate the encapsulation efficiency (EE) (the percentage of drug incorporated into the matrix compared to the initial amount taken for encapsulation) of CCL, 100 mg of CCL was dissolved in 100 mL of water with the help of a bath sonicator for about 5 min. The solution was centrifuged (3000 rpm for 5 min), and the supernatant was analyzed by HPLC. Unbound curcumin, which is free from encapsulation, is insoluble in water and can be separated by centrifugation. The column temperature was kept at 25 °C, the 20 mL sample was injected, and the chromatogram was monitored at 420 nm. The EE was calculated using the following equation:

$$\mathrm{EE} = {W_t}/{W_i} \times 100\%$$

where W_t is the total amount of curcumin in the CCL suspension and W_i is the total quantity of curcumin added initially during preparation.

2.5. In Vitro Release Studies. The in vitro release behavior of curcumin from CCL was determined at pH 6.8 and 3 over a period of 24 h. A known amount of CCL (500 mg) was introduced to the corresponding drug-release medium (500 mL) in the dissolution apparatus and kept agitated at 100 rpm at 37 °C. At a given time (0, 1, 2, 3, 5, 8, and 24 h), an aliquot of the solution was carefully withdrawn and centrifuged and the supernatant solution (1 mL) was made up to 10 mL with acetone. The content of curcumin in the solution was then analyzed by HPLC. A graph was plotted with percentage of curcumin released versus time (Supplementary Figure S2).

2.6. Storage Stability of CCL. Storage stability was assessed by accelerated stability test as per the guidelines of the International Conference on Harmonization (ICH) of technical requirements for the registration of pharmaceuticals for human use.[21] Briefly, the sample packets (10 g) of CCL were sealed in double-layered polyethylene bags and were incubated at 40 ± 2 °C and 70 ± 5% relative humidity for a period of 6 months in a stability chamber (Remi, Mumbai, India). The samples were withdrawn at 0, 1, 2, 3, and 6 months and subjected to various physical and chemical analysis.

2.7. Human Pharmacokinetic Study. In order to elucidate the mechanism of action of CCL in humans, we carried out a pharmacokinetic study on healthy human volunteers following a randomized, double-blind, placebo-controlled, two-arm, two-sequence crossover design. Human study was conducted in accordance with the clinical research guidelines of the Government of India and the Declaration of Helsinki. The protocol was evaluated and approved by an independent ethical committee and was registered in the clinical trial registry of India [CTRI/2020/07/026856, dated 28/07/2020].

Healthy volunteers (N = 15) aged between 24 and 56 years (12 males and 3 females) who were ready to abstain from curcumin-containing food for 2 days prior to the study date were recruited after obtaining a written informed consent. All subjects were nonalcoholic and nonsmokers with average body weight and height of 58 ± 7.5 kg and 170 ± 8.5 cm, respectively. The participants underwent a general physical examination, medical history assessment, and hematological/biochemical analysis to make sure their health is in good condition. Pregnant women, as based on a pregnancy test, were not included. Individuals who participated in a clinical trial in the past 1-month time period and any individual unwilling or unable to comply with the study protocol were also excluded.

During the study day, participants were asked to report at the study center following a ≥10 h overnight fasting and were provided with an oral dose of 2.5 g of CCL/unformulated C95 containing 10.2% of curcuminoids as a ready-to-drink sachet. Each CCL sachet contained 2.5 g of CCL blended with another 3.5 g of CPs in such a way to have a total of 250 mg of curcumin and 5.75 g of CPs. Each C95 sachet was prepared by blending 250 mg of water-soluble curcumin (prepared by mixing 250 mg of C95 with 500 mg of polysorbate 80) with 5.75 g of CPs. Each sachet was suspended in 240 mL of water and consumed for the pharmacokinetic study as reported earlier.[20] Briefly, 2 mL of blood samples was collected into EDTA vacutainers at pre- and various post-administration time intervals of 0, 0.5, 1, 3, 5, 8, and 12 h. Plasma was separated and frozen at −20 °C till analysis. After 1 week of washout period, the subjects were again provided with either unformulated C95 or CCL sachet in a crossover manner as depicted in Figure S1 and plasma was collected and stored as above for curcumin content estimation. From the plasma concentration versus time plot, pharmacokinetic parameters were deduced.

2.8. UPLC-ESI-QqQ-MS/MS Analysis of Curcuminoids in Plasma. Curcumin content in plasma was detected, confirmed, and quantified by UPLC-ESI-QqQ-MS/MS (6460 mass spectrometer, Agilent India Private, Bangalore, India) operated under multiple reaction monitoring (MRM) mode with positive/negative ion polarities, as previously reported.[22] About 1 mL of plasma was extracted with 4 × 5 mL of ethyl acetate, and the ethyl acetate layer was evaporated to dryness at 40 to 45 °C under a nitrogen atmosphere. The residue was then made up to 1 mL with methanol and filtered through a 0.45 μm syringe filter, and 5 μL of this was injected. Separation was achieved with an Eclipse Plus C18 RRHD column (3 × 50 mm; 1.8 μm) and kept at 40 °C, and the mobile phase system consisting of (A) 5 mM ammonium acetate (pH 4.5 adjusted with acetic acid) and (B) acetonitrile containing 0.1% acetic acid, set at a linear gradient of 40 to 80% B within 9 min, was

https://doi.org/10.1021/acsomega.3c02530
ACS Omega 2023, 8, 26243−26252

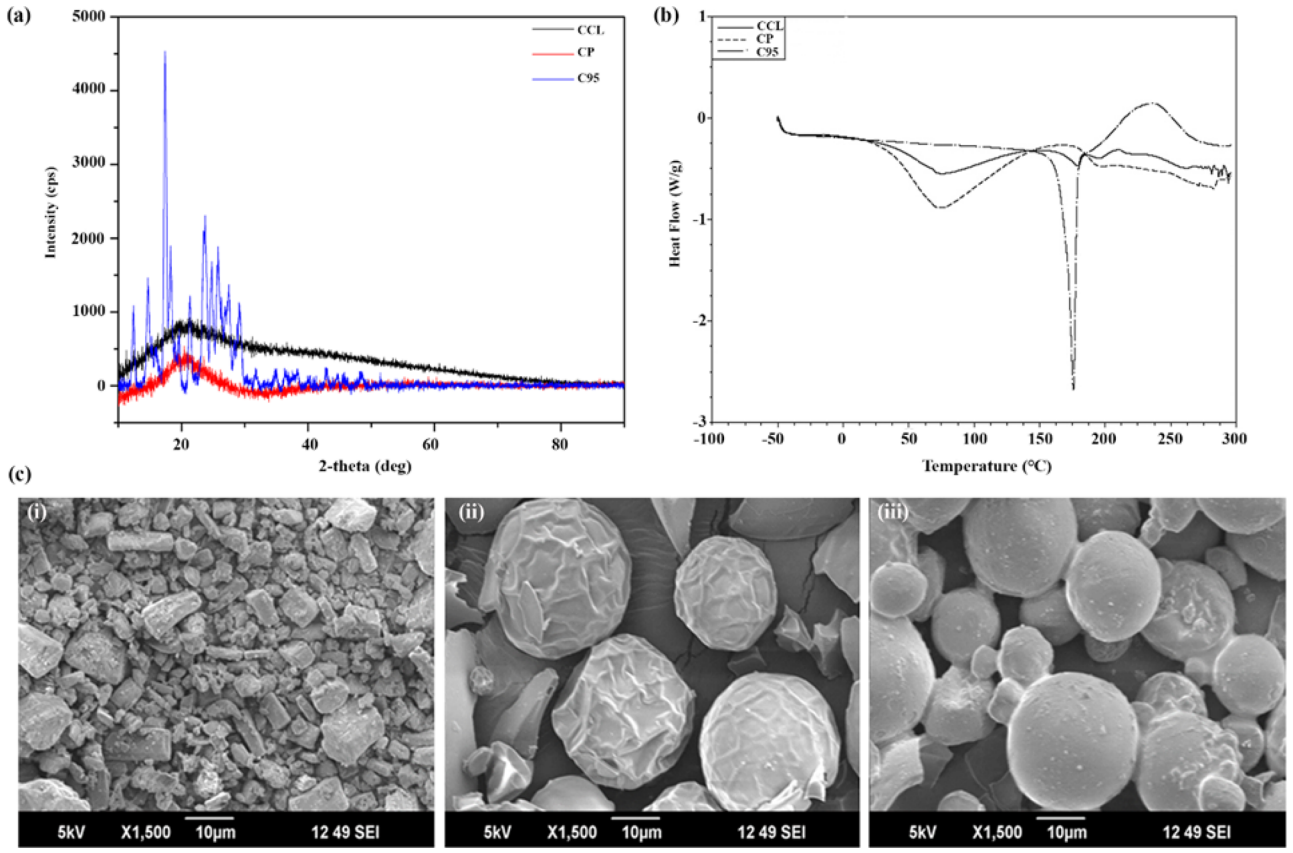

Figure 1. (a) Powder X-ray diffraction patterns of CCL, CP, and C95. (b) DSC thermograms of CCL, CP, and C95. (c) SEM images of (i) C95, (ii) CP, and (iii) CCL.

used. The eluent at a flow rate was 0.3 mL/min and monitored at 425 nm. The Agilent Jet Stream source operated in positive mode with a capillary voltage of 3500 V, 375 °C sheath gas temperature, and 325 °C drying gas temperature was employed for tandem mass spectrometric analysis of curcumin. A positive mode MRM transition of m/z (369.1 → 116.9) for curcumin was recorded. Agilent MassHunter B.7.00 was employed for the data acquisition.

Suitability of MS/MS method was checked by analyzing the blank plasma and curcumin-spiked plasma samples for interference at the respective retention times of each of the analytes. The range and linearity of the extraction efficiency were determined by spiking 50 ng/mL of curcumin in plasma along with the internal standard, salbutamol (50 ng/mL), followed by UPLC/MS/MS analysis on three different days. Matrix-matched calibration curves from plasma were generated by plotting the concentrations of curcumin against peak response and were found to be linear over the concentration range of 1 to 1000 ng/mL, with an R^2 value of 0.9921. The extraction efficiency of curcumin from plasma was found to be greater than 86%, as confirmed by the internal standard. The lower limit of quantification of curcumin was 1 ng/mL.

2.9. Statistical Analysis. Statistical analysis was performed using SPSS (Statistical Package for the Social Science) software version 27 and presented as mean ± standard error. An analysis of variance (ANOVA) followed by Dunnett's test was used to determine the significant difference in plasma pharmacokinetic parameters between the groups. A p-value less than 0.05 was considered statistically significant. All the data processing was performed using GraphPad Prism Version 5.0.

3. RESULTS AND DISCUSSION

3.1. Preparation and Characterization. A water-soluble powder comprising food protein hydrolysates and hydrophobic phytonutrients is of great interest for functional food applications. However, insolubility, instability, and poor bioavailability are always limitations. Herein, we report the supramolecular self-assembly of CPs and curcumin-impregnated phospholipid monolayers to generate surface-modified liposomal microspheres and its solubility, stability, sustained release, and bioavailability. Stabilization of curcumin liposomes in the CP matrix was achieved with good EE (94.67 ± 1.15%) and yield (93.6%) by the spray-drying process. Yield is defined as the percentage of the total input quantity obtained after spray drying.

3.1.1. Physicochemical Properties. The relative physicochemical properties of standard curcumin (C95), CPs, and their formulation CCL are compiled in Table S1. While C95 was a yellow, water-insoluble, crystalline powder (150 ± 25 μm) with a total curcuminoid content of 95.08% (sum of curcumin, DMC, and BDMC) and density of 0.38 g/mL, CP was a colorless, water-soluble, and amorphous powder (125 ± 25 μm) with 0.28 g/mL density. CCL showed 10.2% curcuminoid content and was a yellow, water-soluble, and amorphous powder with a density of 0.29 g/mL. CCL was free-flowing (particles do not stick together), but C95 showed significant aggregation and poor flow property. It was established that the cohesion increases with decreasing size of the powder particles and hence poor flow; particles smaller than 100 μm are generally cohesive.[23]

https://doi.org/10.1021/acsomega.3c02530
ACS Omega 2023, 8, 26243−26252

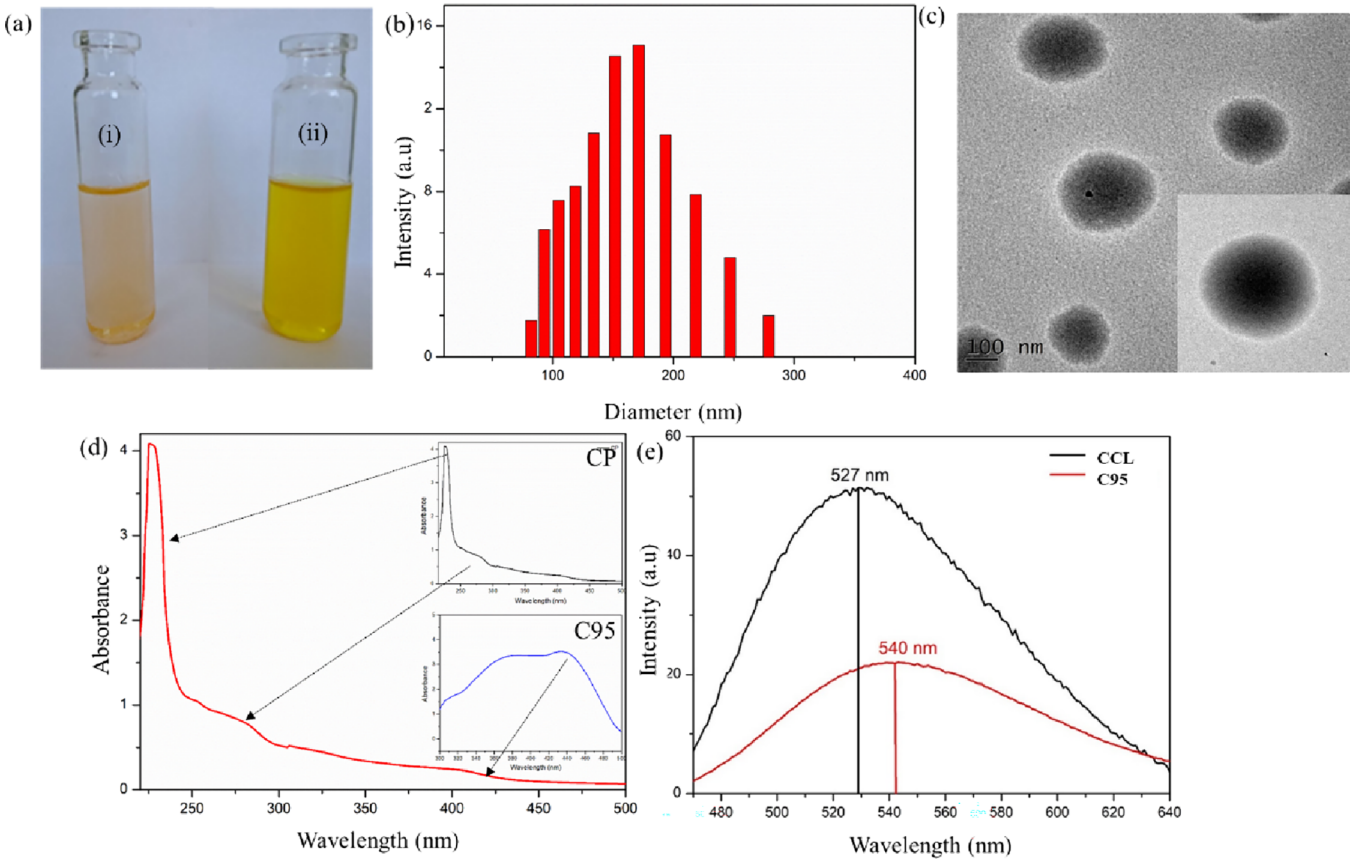

Figure 2. (a) Photograph indicating the solubility of (i) C95 and (ii) CCL in water. (b) Particle size distribution of CCL in water by DLS. (c) TEM image of CCL and the inset figure showing the low-magnification image indicating the nano distribution of CCL. (d) UV−vis absorption spectra of CCL and the inset figures showing the absorption spectra of C95 and CP. (e) Photoluminescence spectra of CCL and C95.

The physical nature and the encapsulation of crystalline curcumin into the collagen network were evident from PXRD, DSC, and SEM analyses (Figure 1). Curcumin (C95) showed well-defined diffraction peaks at 2θ values of 12.1, 14.5, 17.4, 21.3, 24.5, 25.9, 27.5, and 29.2° characteristic of a crystalline material.[24] CP exhibited a broad hump-like pattern around 22°. CCL also provided a typical hill-like plot of an amorphous material with no characteristic sharp peaks of curcumin (Figure 1a), indicating possible encapsulation of curcumin in the lipid/collagen matrix.[25,26] The amorphous nature of CCL was also evident from DSC analysis (Figure 1b). A sharp endothermic shift at 175.74 °C due to its melting was visible for C95. CP showed no sharp peaks, rather a broad hump-like endothermic shift at 74.60 and 194.23 °C. Upon complexation, no sharp peak of C95 was visible in CCL, rather weak endothermic shifts were noticed (74.60 °C → 71.77 °C; 194.23 °C → 196.33 °C; 175.74 °C → 179.49 °C), suggesting the amorphous nature and the adduct formation between the two entities, as reported earlier.[27,28] The surface morphology of C95, CP, and CCL was analyzed by SEM (Figure 1c), which showed the needle-shaped sharp-edged crystals of C95 with irregular morphology, while CP showed amorphous spherical particles with a rough surface. CCL on the other hand showed amorphous and well-ordered spherical nanoparticles with a smooth surface, indicating that the present process is a viable strategy for the encapsulation of crystalline curcumin into the CP network.

Solubility studies indicated enhanced aqueous solubility of curcumin in CCL by 1.46×10^5 times (14 ng/mL for C95 and 2040 μg/mL for CCL) (Figure 2a). The mean particle size of CCL in aqueous solution was found to be ∼176.0 ± 37.4 nm (PDI: 0.206) with a zeta potential of −63.5 ± 1.3 mV when analyzed using the DLS technique (Figure 2b). Further TEM analysis also revealed uniform spherical particles of CCL with less than 200 nm size (Figure 2c).

3.1.2. Ultraviolet/Visible and Fluorescence Spectroscopic Studies. Figure 2d shows the UV−vis absorption spectra of C95, CP, and CCL. C95 exhibited a strong absorption peak around 430 nm due to the $\pi-\pi^*$ transition of the *cis*-enolic form.[29] CP showed two characteristic absorption maxima at 226 and 265 nm. The absorption at 226 nm may be attributed to the polyproline type II framework conformation, and that at 265 nm can be due to the $\pi-\pi^*$ electron transition of aromatic amino acids.[30] CCL on the other hand exhibited a hill-like absorption spectrum spread out from 190 to 500 nm with a significant shift in the characteristic absorption peaks. The absorption maximum of curcumin at 430 nm was shifted to 403 nm, and that of CP at 265 was shifted to 275 nm. The observed shift in curcumin absorption maximum may be due to the complex formation with PL,[31] and the shift observed in CPs can be due to the variations in the microenvironment of the aromatic side chains.[29,30]

Fluorescence spectra of C95 and CCL were recorded at an excitation wavelength of 420 nm, and the corresponding emission was observed at 540 nm for C95 and at 527 nm for CCL (Figure 2e). The blue shift with increased intensity observed for CCL indicates the changes in its microenvironment, resulting from the liposomal formation and further interactions with the CP network. The altered environment due to encapsulation or impregnation can affect the electronic

https://doi.org/10.1021/acsomega.3c02530
ACS Omega 2023, 8, 26243−26252

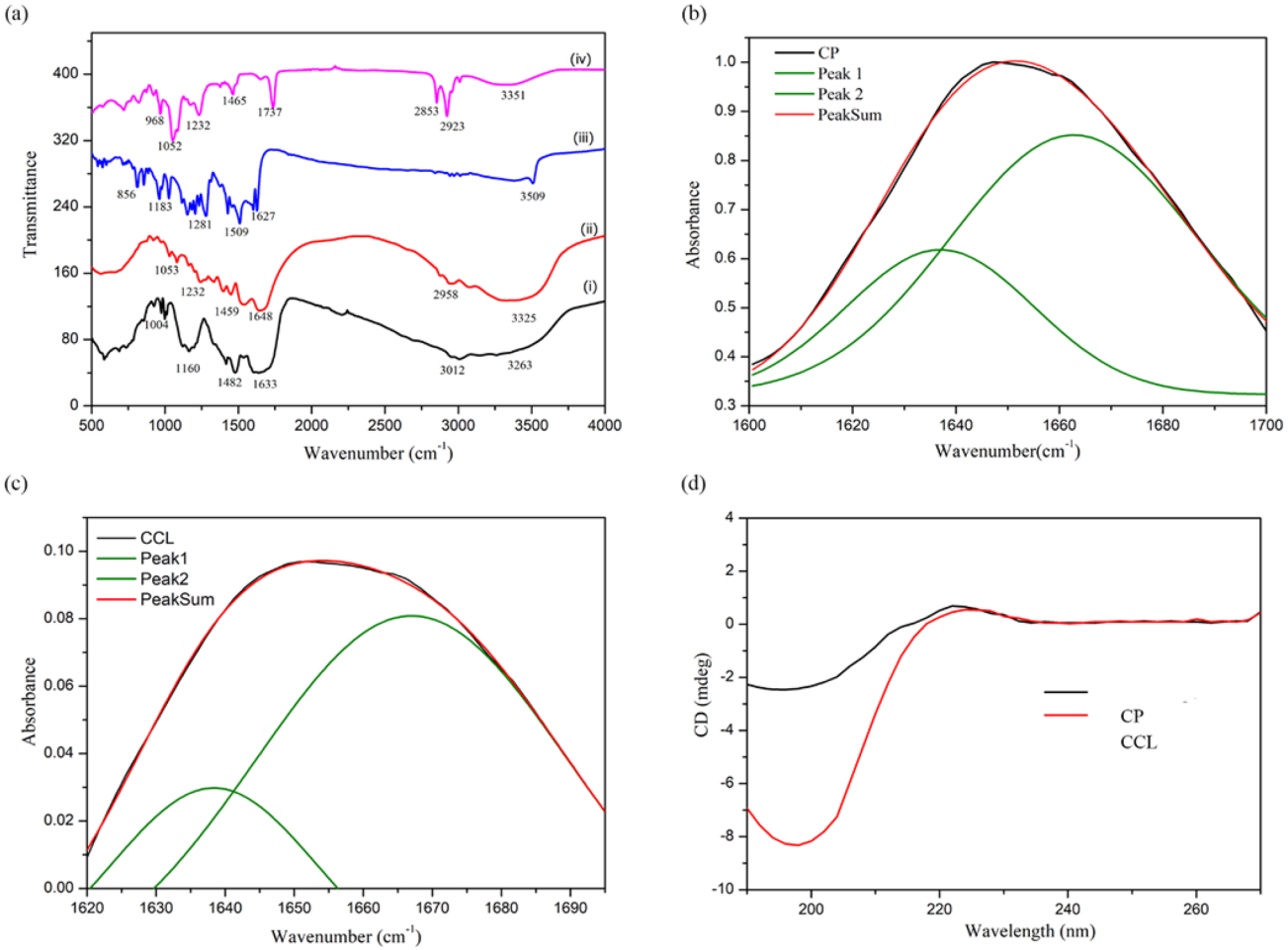

Figure 3. (a) FTIR spectra of (i) CCL, (ii) CP, (iii) C95, and (iv) PL. (b) Deconvoluted FTIR amide I peaks of CP (green lines), indicating an α-helix at 1662 cm^{-1} and a triple helix at 1633 cm^{-1}. (c) Deconvoluted amide I peaks of CCL (green lines), indicating the shift of peaks corresponding to an α-helix at 1638 cm^{-1} and a triple helix at 1667 cm^{-1}. (d) Circular dichroism spectra of CP and CCL.

properties of the curcumin molecule leading to a change in its electronic interactions and emission characteristics.[32,33]

3.1.3. Conformational Analysis of CCL. FTIR spectra of C95, PL, CP, and CCL are shown in Figure 3a. C95 showed all characteristic peaks of curcumin, as reported earlier.[34−36] The peak at 3509 cm^{-1} was attributed to the phenolic O−H stretching vibrations. The peak at 1627 cm^{-1} can be dedicated to the mixed stretching of C═C and C═O. The symmetric aromatic ring stretching vibrations of C═C and C═O were observed around 1602 and 1509 cm^{-1}, respectively. The bands at 1281, 1206, and 1152 cm^{-1} represent the C−O stretching vibrations, and that at 1026 cm^{-1} can be attributed to the C−O−C stretching vibrations. The FTIR spectrum of CP showed all the characteristic bands of a peptide bond and the amino acid proline, as reported earlier.[37,38] The characteristic amide A (N−H stretching) and B (asymmetric CH_2 stretching) bands were observed at 3325 and 2958 cm^{-1}, respectively. The peaks observed at 1648, 1538, and 1242 cm^{-1} were assigned to amide I (C═O stretching), amide II (N−H bending and C−N stretching), and amide III (C−H in plane bending and C−N symmetric stretching) bands, respectively. The peak at 1450 cm^{-1} was assigned to the C−N stretching vibration of cyclic proline, and the $-CH_2$ wagging vibrations of glycine backbone was visible at 1333 cm^{-1}. In the FTIR spectrum of the PL, the peaks at 2853 and 2923 cm^{-1} attributed respectively to the symmetric and asymmetric stretching in the CH_2 groups of the alkyl chain. The broad absorption band around 3550 cm^{-1} was due to the O−H stretching vibrations, and that at 1737 cm^{-1} was assigned to the stretching vibrations of the ester carbonyl groups. The symmetric and asymmetric stretching of PO_2^- were observed around 924 and 1232 cm^{-1} respectively.[35]

FTIR spectra of CCL exhibited the characteristic peaks of both C95 and CP, indicating the inclusion of curcumin in the CP matrix without chemical modifications. However, a significant shift to various peaks was observed which can be assigned to noncovalent interactions such as H-bonding, hydrophobic interactions, and electrostatic interactions among C95, PL, and CP moieties. It was observed that the peaks due to C95 were shifted, indicating the formation of curcumin liposomes, as reported earlier.[35] In CCL, the wavenumbers of amide A and amide B bands of CP were shifted as 3325 → 3263 cm^{-1} and 2958 → 3012 cm^{-1} respectively, and the amide I band was found to be shifted as 1648 → 1633 cm^{-1}. The shifts in amide bands may be attributed to the plausible surface decoration of liposomes by CPs stabilized by the intermolecular H-bonding with the polar head groups of lipids. Such interactions and changes in the amide bands have already been reported.[30,39]

Deconvolution of the amide I band has been recognized as a method to predict the secondary structures in peptides.[40] Deconvolution in CP and CCL revealed two distinguished peaks at 1630 and 1660 cm^{-1} which are respectively ascribed to triple helix and the α-helix conformations (Figure 3b,c).[41] The ratio of

https://doi.org/10.1021/acsomega.3c02530
ACS Omega 2023, 8, 26243−26252

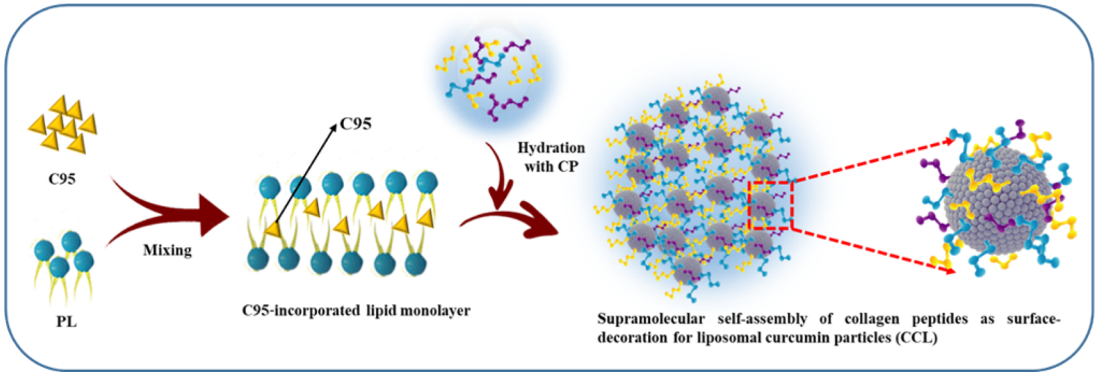

Figure 4. Schematic representation of the two-stage supramolecular self-assembly of collagen peptides, phospholipids, and curcumin leading to the nano-weaving of collagen peptides around the curcumin liposomes to generate collagen peptide-anchored curcumin liposomal complex (CCL).

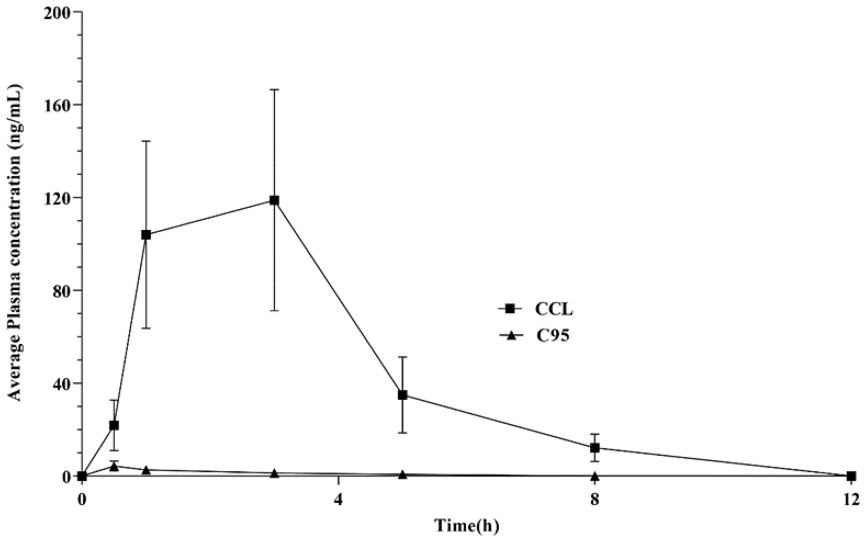

Figure 5. Plasma concentration versus time course following the oral administration of CCL and C95 as sachets (2.5 g powder containing 250 mg of either C95 or CCL). Statistical analysis was performed using SPSS software version 27, and all data points were expressed as mean ± SD. GraphPad Prism Version 5.0 was used to plot the graph.

intensity of these peaks can be used to estimate the degree of secondary conformation. From the ratio of the intensity of the deconvoluted peaks (1630 cm^{-1}/1660 cm^{-1}), the degree of triple helix content has been found to be reduced (<10%) upon CCL formation, indicating a plausible structural alteration of CP probably due to the self-assembly of the peptides around the liposomes.

To further ascertain the changes in the conformation of CP due to the self-assembly of curcumin, PL, and CPs during CCL formation, CD studies at 190 to 300 nm range were carried out. CD spectra of CPs showed a negative minimum at 200 nm and a maximum at 220 nm (Figure 3d). Upon formulation with C95 and PL, the molar ellipticity of CP showed a decrease for 220 nm (positive peak) and an increase for 197 nm (negative peak). The molar ellipticity ratio (Rpn), a ratio of the intensity of the positive and negative peaks, for CP and CCL is 0.07 and 0.28, respectively. Rpn is a characteristic property of the triple helix conformation of collagen and collagen-like peptides.[42] Rpn values of CCL showed a significant increase from those of CP, indicating a conformational change. The increase in Rpn value due to the physical or chemical supramolecular association of CPs has already been reported.[43,44] The conformational variation as observed upon CD studies was in agreement with the FTIR and UV/Vis spectroscopy results, which revealed a shift in amide I band and red shift, respectively. Such variations in the UV/vis spectrum have been dedicated to the micro-environmental change of aromatic amino acid side chains around the polypeptide chain and a helix−coil transition.[30]

Thus, the spectroscopic studies established that curcumin was initially interacting with PL and trapped within the acyl chains through hydrophobic interactions. Upon hydration with the aqueous solution of CP, the curcumin−phospholipid complex interacts with the CPs through noncovalent interactions mediated by intermolecular H-bonding and hydrophobic interactions between the amino acid side chains and acyl chains in the liposomal double layers. The electrostatic force of attraction between the CP and polar head groups of PL was also found to be present. Such interaction leads to a strong adsorption of peptide around the liposome to affect a nanoencapsulation of curcumin through phospholipid−collagen interaction, as pictorially depicted in Figure 4. Two-stage self-assembly leading to a layered structure around the liposome core is clear from the TEM image where it can be observed as dark and light concentric circles (Figure 2c).

3.1.4. In Vitro Release Study. The in vitro release of curcumin from CCL under both stomach and intestinal pH conditions is shown in Figure S2, which indicated a sustained release. The

https://doi.org/10.1021/acsomega.3c02530
ACS Omega 2023, 8, 26243−26252

Table 1. Pharmacokinetic Parameters of CCL and C95 Followed by Supplementation as Sachet

sample	sachet weight[a] (g)	C_{max} (ng/mL)	T_{max} (h)	$T_{1/2}$ (h)	AUC (ng·h/mL)	folds
CCL	2.5	118.84 ± 47.64	3.27 ± 0.70	4.4 ± 0.54	508.6 ± 117.44	51.01
C95	2.5	4.35 ± 2.18	0.53 ± 0.12	0.7 ± 0.15	9.97 ± 3.83	1

[a]2.5 g of sachet contained 250 mg each of either C95 or CCL. C_{max}, maximum plasma concentration; T_{max}, time taken to reach the maximum concentration in plasma; $T_{1/2}$, time taken to reduce the plasma concentration to half of its maximum observed concentration; AUC, area under the curve.

powder form of CCL released almost 22.75% of curcumin at pH 3.0 and 23.01% at pH 6.8, in 24 h.

3.2. Accelerated Stability Study of CCL. Accelerated stability test at 40 ± 2 °C and relative humidity 70 ± 5% have been suggested by ICH as a measure of the storage stability of a drug for human use with a shelf-life of 2 years. The results of the test are shown in Table S2, which revealed no significant degradation for curcumin content. Moreover, the color, particle size, moisture content, and microbial status of CCL were also remained stable during the study period.

3.3. Human Pharmacokinetic Studies of CCL. It has been established that the poor bioavailability of curcumin owing to its insolubility, instability in the gastrointestinal tract, rapid biotransformation, and fast elimination from the systemic circulation is responsible for its clinical insignificance even at a high dosage.[17] Although a number of formulations using various synthetic emulsifiers have been reported, there exist a great demand for natural and green delivery technologies using food components to improve the bioavailability with extended elimination half-life. In the present study, supplementation of CCL (2.5 g of CCL contained 250 mg of curcumin and 1825 mg of CPs) produced a significantly high concentration of curcumin in plasma for 12 h, compared to the unformulated standard curcumin as evident from the plasma concentration versus time plot (Figure 5). From the plot, pharmacokinetic parameters comprising the maximum curcumin concentration in the blood (C_{max}), the time taken to reach the maximum concentration (T_{max}) and the concentration of curcumin in the blood after 12 h (C_{12max}), the area under the curve (AUC), and the elimination half-life ($T_{1/2}$) were calculated (Table 1). From AUC_{0-12h}, it was observed that CCL exhibited 53-fold enhancement in bioavailability of curcumin compared to the standard curcumin (C95). The comparison of C_{max} values indicated 27-fold enhancement in absorption from CCL. Curcumin absorption reached a maximum level after 4.2 h post-administration, and its half-life was 7 h indicating the sustained intestinal release from CCL. The UPLC-ESI-QqQ-MS/MS method in the present study is a well-validated method that has already been shown to be reliable for the estimation of free curcuminoids from biomatrices.[22,45]

CCL was instantly water-soluble and was in a free-flowing granular powder form. When dissolved in water (240 mL), it produced a yellow drink. Volunteers reported no major sensory issues like taste, aroma, or aftertaste of turmeric in the CCL drink, compared to the unformulated standard curcumin (C95) drink, which had strong taste and aroma of turmeric and was extremely difficult to drink. No sugar and flavor were used in sachets of both CCL and C95.

4. CONCLUSIONS

In summary, the present contribution reported a two-stage self-assembly process for the supramolecular rearrangement of curcumin, phospholipids, and CPs to form collagen−peptide-decorated liposomal complexes of curcumin (CCL) with enhanced solubility, stability, and bioavailability suitable for functional food applications. The formulation was achieved by a simple green process (using ethanol and water), without any synthetic emulsifiers or additives. CCL was obtained as free-flowing microspheres with instant cold-water solubility and favorable organoleptic properties suitable for consumption as a beverage. PXRD, DSC, and SEM studies revealed the encapsulation of crystalline curcumin in the CP matrix to form amorphous CCL. Spectroscopic studies using UV−vis, fluorescence, FTIR, and CD established the self-assembly of curcumin in phospholipid bilayers as the liposomal vesicles and further rearrangement of CPs around the lipid layer to act as a matrix for the encapsulation of liposomes. Self-assembly of CPs around the surface of the liposomes was evident from the TEM, which clearly showed a layered structure of the particles. Various noncovalent interactions and conformational changes leading to the supramolecular assembly were further evident from the FTIR and CD studies. Upon human pharmacokinetic studies, CCL exhibited improved bioavailability of curcumin with higher plasma concentration and half-life indicating longer duration of existence in the systemic circulation. Thus, the novelty of the present contribution lies in its simple and scalable green process for the co-delivery of curcumin and CPs at its physiologically relevant dosage/serving in a ready-to-drink form, without taste or aroma issues, for the plausible improved bioactivity. Further studies, including animal and human-intervention studies, are recommended to evaluate the synergistic healing effect due to the co-administration of curcumin along with the CPs in bioavailable form. In general, the formulation opens a green approach for enhancing the solubility and bioavailability of phytonutrients and their co-delivery with peptides.

■ ASSOCIATED CONTENT

Supporting Information

The Supporting Information is available free of charge at https://pubs.acs.org/doi/10.1021/acsomega.3c02530.

Schematic representation of the pharmacokinetic study protocol (Figure S1), in vitro release profile (Figure S2), physicochemical properties of CCL and C95 (Table S1), and the accelerated stability of CCL (Table S2) (PDF)

■ AUTHOR INFORMATION

Corresponding Author

Krishnakumar Illathu Madhavamenon − *R&D Centre, Akay Natural Ingredients, Cochin, Kerala 683561, India;* orcid.org/0000-0003-0594-7650; Phone: +91 484 2686111; Email: krishnakumar.im@akay-group.com; Fax: +91 484 2680891

Authors

Maria Jose Louis − *R&D Centre, Akay Natural Ingredients, Cochin, Kerala 683561, India*

Abhilash Balakrishnan − *R&D Centre, Akay Natural Ingredients, Cochin, Kerala 683561, India*

https://doi.org/10.1021/acsomega.3c02530
ACS Omega 2023, 8, 26243−26252

Ashil Joseph − *R&D Centre, Akay Natural Ingredients, Cochin, Kerala 683561, India*
Prasanth Shanmughan − *R&D Centre, Akay Natural Ingredients, Cochin, Kerala 683561, India*
Balu Maliakel − *R&D Centre, Akay Natural Ingredients, Cochin, Kerala 683561, India*

Complete contact information is available at: https://pubs.acs.org/10.1021/acsomega.3c02530

Author Contributions

K.I.M.: conceptualization, supervision, review—editing. M.J.L. and A.J.: developmental works. P.S.: characterization, original draft. A.B.: pharmacokinetic study. B.M.: review.

Notes

The authors declare the following competing financial interest(s): The process and composition described in the present manuscript are protected by a patent application and are trademarked as PEPTOMESTM by Akay Natural Ingredients, Cochin, India. CurcuLAGENTM is the registered trademark for CCL.

■ ACKNOWLEDGMENTS

The authors thank Dr. Praveen V.K., NIIST, for circular dichroism spectroscopy and Dr. Hassan P.S., BARC, for biophysical studies.

■ REFERENCES

(1) Sahoo, D.; Bandaru, R.; Samal, S. K.; Naik, R.; Kumar, P.; Kesharwani, P.; Dandela, R. Oral Drug Delivery of Nanomedicine. *Theory and Applications of Nonparenteral Nanomedicines*; Elsevier 2021, 181−207. doi: DOI: 10.1016/B978-0-12-820466-5.00009-0.

(2) Homayun, B.; Lin, X.; Choi, H. J. Challenges and Recent Progress in Oral Drug Delivery Systems for Biopharmaceuticals. *Pharmaceutics* **2019**, *11*, 129.

(3) Viswanathan, P.; Muralidaran, Y.; Ragavan, G. Challenges in Oral Drug Delivery: A Nano-Based Strategy to Overcome. *Nanostructures for Oral Medicine*;Elsevier 2017, 173−201. doi: DOI: 10.1016/B978-0-323-47720-8.00008-0.

(4) Lin, C. H.; Chen, C. H.; Lin, Z. C.; Fang, J. Y. Recent Advances in Oral Delivery of Drugs and Bioactive Natural Products Using Solid Lipid Nanoparticles as the Carriers. *J. Food Drug Anal.* **2017**, *25*, 219−234.

(5) Pathak, K.; Raghuvanshi, S. Oral Bioavailability: Issues and Solutions via Nanoformulations. *Clin. Pharmacokinet.* **2015**, *54*, 325−357.

(6) Liu, W.; Zhai, Y.; Heng, X.; Che, F. Y.; Chen, W.; Sun, D.; Zhai, G. *Oral Bioavailability of Curcumin: Problems and Advancements*. 2016, *24* (8), 694−702. doi: DOI: 10.3109/1061186X.2016.1157883.

(7) Betz, G.; Aeppli, A.; Menshutina, N.; Leuenberger, H. In Vivo Comparison of Various Liposome Formulations for Cosmetic Application. *Int. J. Pharm.* **2005**, *296*, 44−54.

(8) Lee, M. K. Liposomes for Enhanced Bioavailability of Water-Insoluble Drugs: *In Vivo* Evidence and Recent Approaches. *Pharmaceutics* **2020**, *12*, 264.

(9) Shariare, M. H.; Noor, H. B.; Khan, J. H.; Uddin, J.; Ahamad, S. R.; Altamimi, M. A.; Alanazi, F. K.; Kazi, M. Liposomal Drug Delivery of Corchorus Olitorius Leaf Extract Containing Phytol Using Design of Experiment (DoE): *In-Vitro* Anticancer and *In-Vivo* Anti-Inflammatory Studies. *Colloids Surf., B* **2021**, *199*, 111543.

(10) Lai, W.-F.; Wong, W.-T. Design and Optimization of Quercetin-Based Functional Foods. *Crit. Rev. Food Sci. Nutr.* **2021**, *62*, 7319−7335.

(11) Li, R.; Lin, Z.; Zhang, Q.; Zhang, Y.; Liu, Y.; Lyu, Y.; Li, X.; Zhou, C.; Wu, G.; Ao, N.; Li, L. Injectable and in Situ-Formable Thiolated Chitosan-Coated Liposomal Hydrogels as Curcumin Carriers for Prevention of *in Vivo* Breast Cancer Recurrence. *ACS Appl. Mater. Interfaces* **2020**, *12*, 17936−17948.

(12) Joseph, A.; Balakrishnan, A.; Shanmughan, P.; Maliakel, B.; Illathu Madhavamenon, K. Micelle/Hydrogel Composite as a "Natural Self-Emulsifying Reversible Hybrid Hydrogel (N'SERH)" Enhances the Oral Bioavailability of Free (Unconjugated) Resveratrol. *ACS Omega* **2022**, *7*, 12835−12845.

(13) Joseph, A.; Kumar, D.; Balakrishnan, A.; Shanmughan, P.; Maliakel, B.; Krishnakumar, I. M. Surface-Engineered Liposomal Particles of Calcium Ascorbate with Fenugreek Galactomannan Enhanced the Oral Bioavailability of Ascorbic Acid: A Randomized, Double-Blinded, 3-, Crossover StudySequence. *RSC Adv.* **2021**, *11*, 38161−38171.

(14) Wickremasinghe, N. C.; Kumar, V. A.; Hartgerink, J. D. Two-Step Self-Assembly of Liposome-Multidomain Peptide Nanofiber Hydrogel for Time-Controlled Release. *Biomacromolecules* **2014**, *15*, 3587−3595.

(15) Kunnumakkara, A. B.; Anand, P.; Aggarwal, B. B. Curcumin Inhibits Proliferation, Invasion, Angiogenesis and Metastasis of Different Cancers through Interaction with Multiple Cell Signaling Proteins. *Cancer Lett.* **2008**, *269*, 199−225.

(16) Fuloria, S.; Mehta, J.; Chandel, A.; Sekar, M.; Rani, N. N. I. M.; Begum, M. Y.; Subramaniyan, V.; Chidambaram, K.; Thangavelu, L.; Nordin, R.; Wu, Y. S.; Sathasivam, K. V.; Lum, P. T.; Meenakshi, D. U.; Kumarasamy, V.; Azad, A. K.; Fuloria, N. K. A Comprehensive Review on the Therapeutic Potential of Curcuma Longa Linn. in Relation to Its Major Active Constituent Curcumin. *Front. Pharmacol.* **2022**, *13*, 820806.

(17) Cas, M. D.; Ghidoni, R. Dietary Curcumin: Correlation between Bioavailability and Health Potential. *Nutrients* **2019**, *11*, 2147.

(18) Thomas, J. V.; Smina, T. P.; Khanna, A.; Kunnumakkara, A. B.; Maliakel, B.; Mohanan, R.; Krishnakumar, I. M. Influence of a Low-Dose Supplementation of Curcumagalactomannoside Complex (CurQfen) in Knee Osteoarthritis: A Randomized, Open-Labeled, Active-Controlled Clinical Trial. *Phytother Res.* **2021**, *35*, 1443−1455.

(19) León-López, A.; Morales-Peñaloza, A.; Martínez-Juárez, V. M.; Vargas-Torres, A.; Zeugolis, D. I.; Aguirre-Álvarez, G. Hydrolyzed Collagen—Sources and Applications. *Molecules* **2019**, *24*, 4031.

(20) Ohnishi, N.; Yamamoto, E.; Tomida, H.; Hyodo, K.; Ishihara, H.; Kikuchi, H.; Tahara, K.; Takeuchi, H. Rapid Determination of the Encapsulation Efficiency of a Liposome Formulation Using Column-Switching HPLC. *Int. J. Pharm.* **2013**, *441*, 67−74.

(21) ICH. *ICH Topic Q 1 A (R2) Stability Testing of New Drug Substances and Products Step 5 Note for Guidance on Stability Testing: Stability Testing Of New Drug Substances And Products*; ICH 2003. http://www.emea.eu.int.

(22) Kumar, D.; Jacob, D.; Subash, P. S.; Maliakkal, A.; Johannah, N. M.; Kuttan, R.; Maliakel, B.; Konda, V.; Krishnakumar, I. M. Enhanced Bioavailability and Relative Distribution of Free (Unconjugated) Curcuminoids Following the Oral Administration of a Food-Grade Formulation with Fenugreek Dietary Fibre: A Randomised Double-Blind Crossover Study. *J. Funct. Foods.* **2016**, *22*, 578−587.

(23) Šimek, M.; Grünwaldová, V.; Kratochvíl, B. Comparison of Compression and Material Properties of Differently Shaped and Sized Paracetamols. *Kona Powder Part. J.* **2017**, *34*, 197−206.

(24) Singh, P. K.; Wani, K.; Kaul-Ghanekar, R.; Prabhune, A.; Ogale, S. From Micron to Nano-Curcumin by Sophorolipid Co-Processing: Highly Enhanced Bioavailability, Fluorescence, and Anti-Cancer Efficacy. *RSC Adv.* **2014**, *4*, 60334−60341.

(25) Yang, X.; Li, Z.; Wang, N.; Li, L.; Song, L.; He, T.; Sun, L.; Wang, Z.; Wu, Q.; Luo, N.; Yi, C.; Gong, C. Curcumin-Encapsulated Polymeric Micelles Suppress the Development of Colon Cancer *In Vitro* and *In Vivo*. *Sci. Rep.* **2015**, *5*, 1−15.

(26) Zabihi, F.; Xin, N.; Jia, J.; Chen, T.; Zhao, Y. High Yield and High Loading Preparation of Curcumin−PLGA Nanoparticles Using a Modified Supercritical Antisolvent Technique. *Ind. Eng. Chem. Res.* **2014**, *53*, 6569−6574.

(27) Karri, V. V. S. R.; Kuppusamy, G.; Talluri, S. V.; Mannemala, S. S.; Kollipara, R.; Wadhwani, A. D.; Mulukutla, S.; Raju, K. R. S.;

Malayandi, R. Curcumin Loaded Chitosan Nanoparticles Impregnated into Collagen-Alginate Scaffolds for Diabetic Wound Healing. *Int. J. Biol. Macromol.* **2016**, *93*, 1519−1529.
(28) Samouillan, V.; Delaunay, F.; Dandurand, J.; Merbahi, N.; Gardou, J.-P.; Yousfi, M.; Gandaglia, A.; Spina, M.; Lacabanne, C. The Use of Thermal Techniques for the Characterization and Selection of Natural Biomaterials. *J. Funct. Biomater.* **2011**, *2*, 230−248.
(29) Jutkova, A.; Chorvat, D.; Miskovsky, P.; Jancura, D.; Datta, S. Encapsulation of Anticancer Drug Curcumin and Co-Loading with Photosensitizer Hypericin into Lipoproteins Investigated by Fluorescence Resonance Energy Transfer. *Int. J. Pharm.* **2019**, *564*, 369−378.
(30) Kanungo, I.; Fathima, N. N.; Jonnalagadda, R. R.; Nair, B. U. Go Natural and Smarter: Fenugreek as a Hydration Designer of Collagen Based Biomaterials. *Phys. Chem. Chem. Phys.* **2015**, *17*, 2778−2793.
(31) Othman, A. K.; el Kurdi, R.; Badran, A.; Mesmar, J.; Baydoun, E.; Patra, D. Liposome-Based Nanocapsules for the Controlled Release of Dietary Curcumin: PDDA and Silica Nanoparticle-Coated DMPC Liposomes Enhance the Fluorescence Efficiency and Anticancer Activity of Curcumin. *RSC Adv.* **2022**, *12*, 11282−11292.
(32) Ghatak, C.; Rao, V. G.; Mandal, S.; Ghosh, S.; Sarkar, N. An Understanding of the Modulation of Photophysical Properties of Curcumin inside a Micelle Formed by an Ionic Liquid: A New Possibility of Tunable Drug Delivery System. *J. Phys. Chem. B* **2012**, *116*, 3369−3379.
(33) Prabu, S.; Mohamad, S. Curcumin/Beta-Cyclodextrin Inclusion Complex as a New "Turn-off" Fluorescent Sensor System for Sensitive Recognition of Mercury Ion. *J. Mol. Struct.* **2020**, *1204*, No. 127528.
(34) Bechnak, L.; Khalil, C.; el Kurdi, R.; Khnayzer, R. S.; Patra, D. Curcumin Encapsulated Colloidal Amphiphilic Block Co-Polymeric Nanocapsules: Colloidal Nanocapsules Enhance Photodynamic and Anticancer Activities of Curcumin. *Photochem. Photobiol. Sci.* **2020**, *19*, 1088−1098.
(35) Hasan, M.; Ben Messaoud, G.; Michaux, F.; Tamayol, A.; Kahn, C. J. F.; Belhaj, N.; Linder, M.; Arab-Tehrany, E. Chitosan-Coated Liposomes Encapsulating Curcumin: Study of Lipid−Polysaccharide Interactions and Nanovesicle Behavior. *RSC Adv.* **2016**, *6*, 45290−45304.
(36) Zhang, D.; Jiang, F.; Ling, J.; Ouyang, X. K.; Wang, Y. G. Delivery of Curcumin Using a Zein-Xanthan Gum Nanocomplex: Fabrication, Characterization, and in Vitro Release Properties. *Colloids Surf., B* **2021**, *204*, 111827.
(37) Silva, Z. S.; Botta, S. B.; Ana, P. A.; França, C. M.; Fernandes, K. P. S.; Mesquita-Ferrari, R. A.; Deana, A.; Bussadori, S. K. Effect of Papain-Based Gel on Type I Collagen - Spectroscopy Applied for Microstructural Analysis. *Sci. Rep.* **2015**, *5*, 1−7.
(38) de Campos Vidal, B.; Mello, M. L. S. Collagen Type I Amide I Band Infrared Spectroscopy. *Micron* **2011**, *42*, 283−289.
(39) Wang, X.; Zhang, Z.; Xu, H.; Li, X.; Hao, X. Preparation of Sheep Bone Collagen Peptide−Calcium Chelate Using Enzymolysis-Fermentation Methodology and Its Structural Characterization and Stability Analysis. *RSC Adv.* **2020**, *10*, 11624−11633.
(40) Belbachir, K.; Noreen, R.; Gouspillou, G.; Petibois, C. Collagen Types Analysis and Differentiation by FTIR Spectroscopy. *Anal. Bioanal. Chem.* **2009**, *395*, 829−837.
(41) Terzi, A.; Storelli, E.; Bettini, S.; Sibillano, T.; Altamura, D.; Salvatore, L.; Madaghiele, M.; Romano, A.; Siliqi, D.; Ladisa, M.; de Caro, L.; Quattrini, A.; Valli, L.; Sannino, A.; Giannini, C. Effects of Processing on Structural, Mechanical and Biological Properties of Collagen-Based Substrates for Regenerative Medicine. *Sci. Rep.* **2018**, *8*, 1429.
(42) Feng, Y.; Melacini, G.; Taulane, J. P.; Goodman, M. Acetyl-Terminated and Template-Assembled Collagen-Based Polypeptides Composed of Gly-Pro-Hyp Sequences. 2. Synthesis and Conformational Analysis by Circular Dichroism, Ultraviolet Absorbance, and Optical Rotation. *J. Am. Chem. Soc.* **1996**, *118*, 10351−10358.
(43) Nishad Fathima, N.; Balaraman, M.; Raghava Rao, J.; Unni Nair, B. Effect of Zirconium (IV) Complexes on the Thermal and Enzymatic Stability of Type I Collagen. *J. Inorg. Biochem.* **2003**, *95*, 47−54.
(44) Menezes, M. D. L. L. R.; Ribeiro, H. L.; Flávia de Oliveira, M.; de Andrade Feitosa, J. P. Optimization of the Collagen Extraction from Nile Tilapia Skin (*Oreochromis niloticus*) and Its Hydrogel with Hyaluronic Acid. *Colloids Surf., B* **2020**, *189*, 110852.
(45) Krishnakumar, I. M.; Maliakel, A.; Gopakumar, G.; Kumar, D.; Maliakel, B.; Kuttan, R. Improved Blood−Brain-Barrier Permeability and Tissue Distribution Following the Oral Administration of a Food-Grade Formulation of Curcumin with Fenugreek Fibre. *J. Funct. Foods.* **2015**, *14*, 215−225.

https://doi.org/10.1021/acsomega.3c02530
ACS Omega 2023, 8, 26243−26252